AFRL-DE-PS-
TP-2006-1013

AFRL-DE-PS-
TP-2006-1013

Final Testing and Evaluation of a Meter-Class Actively Controlled Membrane Mirror (Preprint)

Brian Patrick, et al.

13 April 2006

Journal Article

AIR FORCE RESEARCH LABORATORY
Directed Energy Directorate
3550 Aberdeen Ave SE
AIR FORCE MATERIEL COMMAND
KIRTLAND AIR FORCE BASE, NM 87117-5776

REPORT DOCUMENTATION PAGE

Form Approved
OMB No. 0704-0188

1. REPORT DATE *(DD-MM-YYYY)*	2. REPORT TYPE	3. DATES COVERED *(From - To)*
13 April 2006	Journal Article (Preprint)	March 2003 - August 2006

4. TITLE AND SUBTITLE

Final Testing and Evaluation of a Meter-Class Actively Controlled Membrane Mirror (Preprint)

5a. CONTRACT NUMBER
F29601-03-C-0040

5b. GRANT NUMBER

5c. PROGRAM ELEMENT NUMBER
65502F

6. AUTHOR(S)

B. Patrick, J. Moore, S. Chodimella, D. Marker, B. deBlonk

5d. PROJECT NUMBER
3005

5e. TASK NUMBER
DP

5f. WORK UNIT NUMBER
BE

7. PERFORMING ORGANIZATION NAME(S) AND ADDRESS(ES)

SRS Technologies
500 Discovery Drive
Huntsville, AL 35806

8. PERFORMING ORGANIZATION REPORT NUMBER

9. SPONSORING / MONITORING AGENCY NAME(S) AND ADDRESS(ES)
Air Force Research Laboratory
3550 Aberdeen Avenue SE
Kirtland AFB, NM 87117-5776

10. SPONSOR/MONITOR'S ACRONYM(S)
AFRL/DESE

11. SPONSOR/MONITOR'S REPORT NUMBER(S)
AFRL-DE-PS-TP-2006-1013

12. DISTRIBUTION / AVAILABILITY STATEMENT

Approved for Public Release; Distribution is Unlimited.

13. SUPPLEMENTARY NOTES
Submitted for publication in 7th AIAA Gossamer Spacecraft Forum, Newport, RI, 1-4 May 2006.
GOVERNMENT PURPOSE RIGHTS

14. ABSTRACT
Testing has been completed of a 0.70 meter diameter mirror using thin-film polymer membranes. Advances in polymer film science have resulted in polymer membranes less than 24 microns in thickness with excellent surface roughness and sub wavelength thickness variation. Because of such high quality material production, this has allowed the concept of a lenticular mirror design to be reconsidered. This involves the use of a clear canopy integrated with a reflectively coated membrane and pressurization is used to establish a desired focal length. Boundary errors as well as significant spherical aberration are typical aberrations associated with such a mirror system. The membrane mirror described here accounts for these errors by utilizing an active boundary control system to help alleviate any errors near the boundary due to possible uneven stresses and any mounting errors. A varied stress coating is also deposited onto the reflective polymer membrane to alter the mechanical properties of the film, that when pressurized it pushes more towards a parabola instead of a severely aberrated aspheric mirror. The final test data obtained on this system is presented in this paper.

15. SUBJECT TERMS

16. SECURITY CLASSIFICATION OF:			17. LIMITATION OF ABSTRACT	18. NUMBER OF PAGES	19a. NAME OF RESPONSIBLE PERSON
a. REPORT	b. ABSTRACT	c. THIS PAGE	SAR	15	Ryan Conk
Unclassified	Unclassified	Unclassified			19b. TELEPHONE NUMBER *(include area code)*

Final Testing and Evaluation of a Meter-Class Actively Controlled Membrane Mirror

B. Patrick*, J. Moore†, and S. Chodimella‡
SRS Technologies, Huntsville, AL, 35806

D. Marker§, and B. deBlonk**
Air Force Research Lab, Albuquerque, NM, 87117

Testing has been completed of a 0.70 meter diameter mirror using thin-film polymer membranes. Advances in polymer film science have resulted in polymer membranes less than 24 microns in thickness with excellent surface roughness and sub wavelength thickness variation. Because of such high quality material production, this has allowed the concept of a lenticular mirror design to be reconsidered. This involves the use of a clear canopy integrated with a reflectively coated membrane and pressurization is used to establish a desired focal length. Boundary errors as well as significant spherical aberration are typical aberrations associated with such a mirror system. The membrane mirror described here accounts for these errors by utilizing an active boundary control system to help alleviate any errors near the boundary due to possible uneven stresses and any mounting errors. A varied stress coating is also deposited onto the reflective polymer membrane to alter the mechanical properties of the film, that when pressurized it pushes more towards a parabola instead of a severely aberrated aspheric mirror. The final test data obtained on this system is presented in this paper.

I. Introduction

TEST results are presented in this paper that have resulted from the development and optimization of a pressure augmented membrane mirror system consisting of a thin-film polymer material. A 0.70m diameter test article is shown in Fig. 1. This mirror consists of a reflective-coated polymer membrane to serve as the mirror surface and a clear polymer membrane to serve as the canopy. The films are secured to mounting rings and sealed together forming a lenticular structure in which a positive pressure can be applied from a precision regulated supply to inflate the system to achieve a desired focal length. The use of inflation pressure to introduce curvature and rigidize a stretched membrane to form a mirror has been explored in the past[1]. Such lenticular structures have been successfully used for solar concentrators and other non imaging applications[2]. However, the lack of optical quality transparent membrane canopies has made such a concept impractical for imaging systems. This problem has been solved by the development of highly specular films with sub wavelength thickness variation manufactured using CP1-DE transparent polyimide material[3]. An additional complication also arises from the fact that the characteristic shape of an inflated flat membrane, with fixed boundary conditions, is not parabolic[1]. The focal length of an inflated membrane is longer near the center and shorter at the edges. The aberration is primarily due to 1st order spherical aberration. The results presented in this paper address the feasibility of correcting the characteristic pressurized shape error as well as other typical aberrations through use of an active boundary control system and controlled material depositions onto the membrane surface.

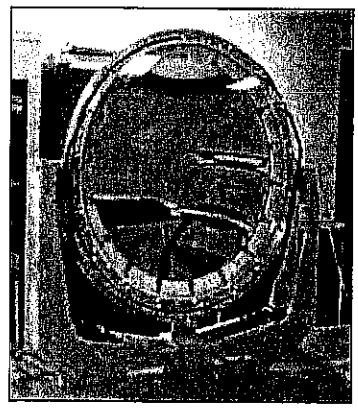

Figure 1. 0.70m Membrane Mirror.

* Optical Engineer, Aerospace Technologies, 500 Discovery Dr.
† Aerospace Director, Aerospace Technologies, 500 Discovery Dr.
‡ Engineer, Aerospace Technologies, 500 Discovery Dr.
§ Program Director, AFRL/DEBS
** Program Director, AFRL/DEBS

One of the primary objectives of using the pressurized lenticular system is to reduce the overall weight of large aperture imaging systems. The ideal minimum weight mirror design consists of a thin unsupported membrane of the minimum thickness required to reflect photons. However, some structure will be required for deploying and supporting any membrane mirror. In the simplest form this could amount to a simple rigid planar boundary. On the other end of the spectrum some form of full aperture control could be considered; however, there is a greater weight penalty for this design. A more attractive alternative is the intermediate solution of developing an adaptively controlled active boundary. The scaling relationship for an adaptive boundary is favorable.

II. Mount Design and Fabrication

Studies previously conducted[4] have shown that active boundary control can be very effective for correcting certain types of figure errors typically seen in membrane mirrors while maintaining traceability to lightweight systems. Of the various active boundary control configurations evaluated, the best performance was achieved by a design that used a combination of out-of-plane boundary warping and electrostatic pressure actuators located circumferentially around the outer diameter of the membrane just inside the boundary support ring. Almost 100% correction of the simulated coma and astigmatism was predicted with this configuration with finite element modeling and similar results were shown from actual test data on the small-scale mount (radial actuators instead of electrostatic, but the effect is similar). The 0.70m mirror mount discussed here utilizes electrostatic pressure control (capable of 18 electrostatic force actuators located circumferentially around the outer 1 inch of the membrane outer diameter) coupled with boundary warping (32 out-of-plane normal actuators) to demonstrate the feasibility of boundary control.

The test article design is a 0.70m diameter clear aperture parabolic mirror set at an f/2.25. The mirror is formed by pressurizing a flat isotropic CP1-DE membrane mounted in a planar circular reflector ring. The magnitude of pressure required to inflate the flat membrane to an f/2.25 parabolic mirror depends on the amount of tensile stress in the membrane. The membrane is assumed to have an intrinsic tensile stress (pre-stress) during the curing process, due to CTE mismatch between it and the casting substrate. Low CTE polymers are a potential option for such a system if athermalization is required. The system consists of a canopy and mirror film supported by rings that connect and seal together to support a pressure. The membrane mirror is placed against a contact ring that defines the membrane boundary. A reaction ring is used to support the normal actuators as they push against the boundary ring. The boundary ring itself is supported by 18 rods around the diameter and can be lowered further against the membrane mirror simply by reducing the number of precision shims on these support rods. This is available in order to compensate for any reduction of initial stress of the membrane mirror. Active boundary control using electrostatic pressure is achieved by having electrodes on both sides of the reflector membrane, located circumferentially on a 1-inch annulus. The electrodes should be parallel to the membrane after inflation to apply uniform pressure control. Provisions for changing the distance between the electrodes and membrane was also added to ensure adjustment capabilities in case the electrode force cannot be varied as required by adjusting the voltage alone. The electrodes themselves consist of copper panels adhered to Kapton film adhesively attached to the support structure. Figure 2 shows each ring with the electrode patches already in place. The ring wound up being 1/8" thick ceramic doped plastic manufactured using stereolithography (STL). The electrode patches were secured using pressure sensitive adhesive (PSA). Figure 3 shows several images of the mount during final assembly.

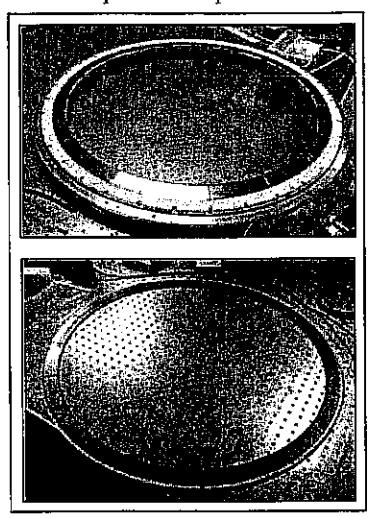

Figure 2. Top and bottom electrode support rings with pads in place.

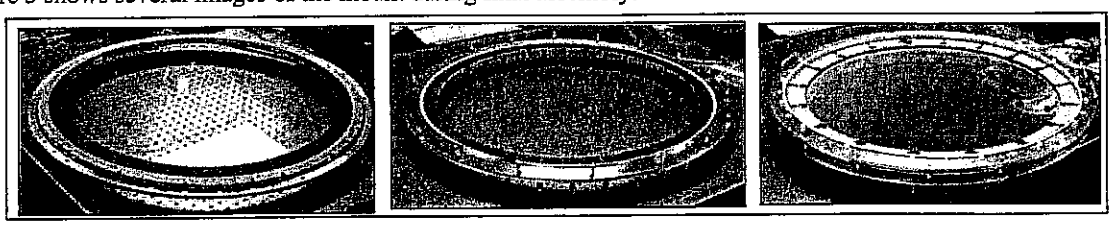

Figure 3. Mirror mount at various stages of assembly.

CP1-DE membranes were produced for integration with the reflector and canopy rings described. Excellent results were obtained on the thickness variation for these films. Four membranes were manufactured for the mirror side. One was applied with a uniform coating and two were applied with a varied stress coating. The remaining membrane was used for internal testing with no coating.

III. Electrostatic Control System Design and Evaluation

A. Initial Modeling and Small-Scale Testing

As stated the 0.70-meter Pressure Augmented Membrane Mirror (PAMM) incorporates radial membrane control by using electrostatic pressure actuators located circumferentially around the outer diameter of the membrane just inside of the boundary support ring. Since electrostatic control can only pull on the membrane, the 0.70-meter mount was designed to have electrodes placed on both sides of the mirror surface to be able to push and pull on the mirror. Though a total of thirty-six electrodes are needed to achieve the necessary surface accuracy in the mirror, only eighteen power supplies are necessary to provide the high voltage. Two connector boxes with 9 sockets in each was designed, where one end of each socket is soldered to the high voltage lead coming from a power supply and a wire from either an electrode on the inner ring or the outer ring can be plugged into the other end. Gaps between sockets and any open metal parts were filled with a dielectric to increase the breakdown voltage. Wider spacing distance was allowed where possible without losing any compactness in the design.

The LabView control software (Fig. 4) was modified and a National Instruments analog output card was setup to accommodate the four additional power supplies mounted in the existing desktop rack system. In addition to the proportional master slider to control voltages on all electrodes, checkboxes are provided in order to select channels to form into groups. Channels in each group can be collectively controlled using proportional group sliders.

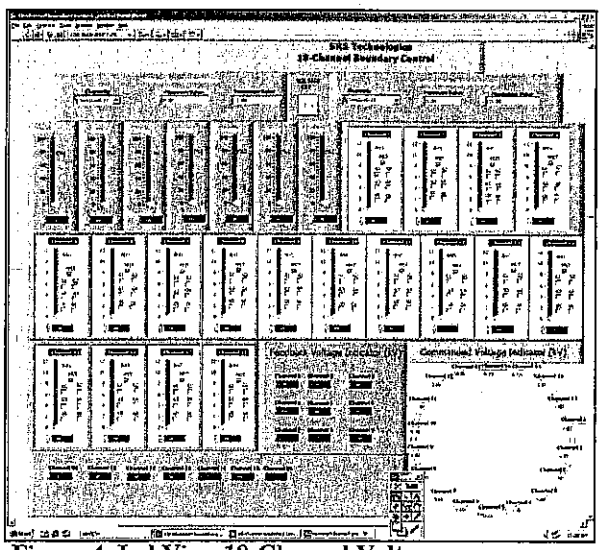

Figure 4. LabView 18-Channel Voltage Control Panel.

The software and control equipment used to control the boundary of the 0.70m was setup and tested by applying it to a full aperture control on the 0.25m prototype mirror already fabricated by SRS. In order to properly test the control software modeling was required to analyze any resulting data and determine the correct voltage settings to offset any measured errors. Analysis and testing have shown that a flat homogenous membrane of uniform thickness will deform into a shape that can be described as a parabolic reflector with significant spherical aberrations. Preliminary analysis has shown that global shape control could possibly be used to reduce RMS surface figure error and spherical aberrations.

A finite element model of a flat membrane was created using Algor non-linear analysis software. The membrane modeled was made of CP1 material, had a 0.25-meter diameter, uniform thickness of 8 microns with a pre-stress of 4060 psi. Pinned boundary conditions were applied all around the circumference of the membrane. The properties for the material used in the analysis were; elastic modulus of 315000 psi, density of 1.341e-4 lb/in^3, Poisson's ratio of 0.34, and a shear modulus of 117537 psi. 864 four-node quadrilaterals with shell element formulation were used to model the membrane. Each node had six degrees of freedom and the whole model consisted of 5190 degrees of freedom.

A 14-channel electrode configuration was evaluated in this small-scale study. In order to individually control each channel in the analysis, the membrane model was divided into 14 groups as shown in Fig. 5. A normal pressure

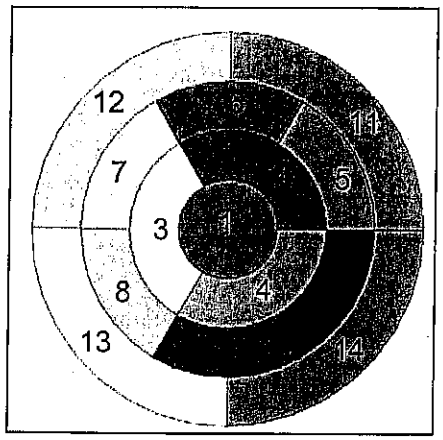

Figure 5. 14-Channel Electrode Layout.

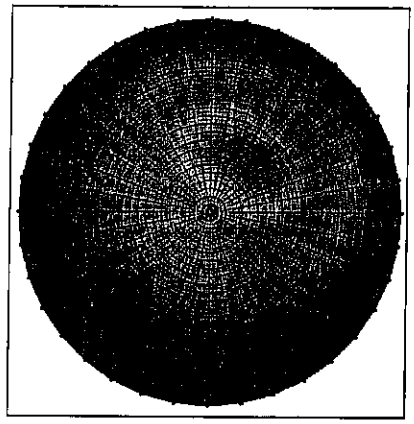

Figure 6. Influence Function of Electrode 2

of 0.040 psi was applied to deform the membrane to an f/3.5 paraboloid. This deformed shape of the mirror is defined as the reference shape. The actuator influence functions are generated by fixing all but one of the actuators in the baseline nominal state, and then calculating the displacements caused by a unit activation (0.001 psi, in this case) of the active actuator. The reference shape is then subtracted from the actuator influence functions to generate the influence function matrix. Once the influence function matrix is generated, a linear least squares algorithm in IODA[5] is used to solve for the combination of actuator positions that minimizes the RMS surface figure error. Figure 6 shows the influence function of electrode 2 after subtracting the reference shape. The feasibility of the global shape control concept was evaluated based on the effective correction obtained on a typical set of random zernike aberrations. Figure 7 shows the random aberration case to be corrected with the 14-channel electrode configuration. Figure 8 illustrates the results from this design evaluation. The RMS surface error was reduced from 5.87 microns to 2.19 microns and the model predicts almost 71% correction of the simulated spherical aberration. After masking the boundary of the membrane as shown in Fig. 9, the RMS surface error further reduced to 0.89 microns and 97% correction of spherical aberration was obtained. Figure 10 summarizes the results from this initial performance evaluation study.

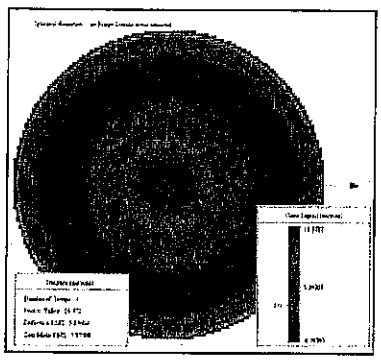

Figure 7. Induced Aberration.

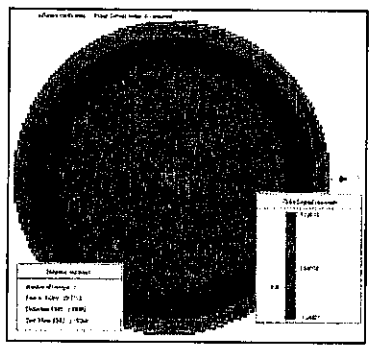

Figure 8. Residual Surface.

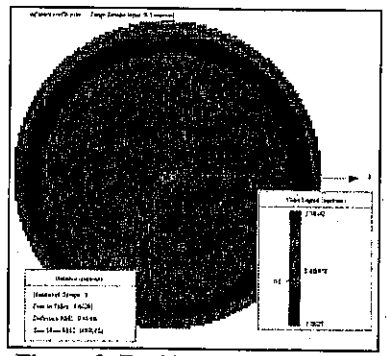

Figure 9. Residual Surface after Masking Boundary.

This simple analysis showed that full aperture control can be effective in decreasing RMS surface figure error and reducing spherical aberrations, therefore this provided an excellent test for the control system and software to be applied later to the large-scale mount which utilizes such control only along the edge of the aperture.

The small scale MANS 25cm clear aperture mount with radial and boundary warping control used in this study is shown in Fig. 11 along with the integration of the electrostatic control hardware and the small scale mount to form the global shape controlled mirror.

Units: Microns	Random aberration Case	Residual surface	% Correction	Residual after masking boundary	% Correction
P-V	19.772	10.3712	**47.5**	4.60291	**76.7**
RMS	5.87598	2.19264	**62.6**	0.898452	**84.7**
Spherical aberration	13.1879	3.75895	**71.5**	0.414797	**96.8**

Figure 10 Performance Evaluation for 14-Channel Electrode Configuration.

B. Electrode Design

The finite element analysis described above supported the electrode design for the large-scale system. Figure 12 shows the electrode configuration mounted behind the mirror. The function of an electrode is to provide a conductive surface where the voltage can be individually controlled independent of other electrodes. The electrode design layout consisted of a 50 micron Kapton vacuum-deposited aluminum film that was cut into size of each group. Small tabs extended from each electrode to transmit voltage from the high-voltage leads to the electrode surface. Insulating gaps between electrodes were created by manually stripping 2.54 mm wide aluminum all around the edge of each electrode.

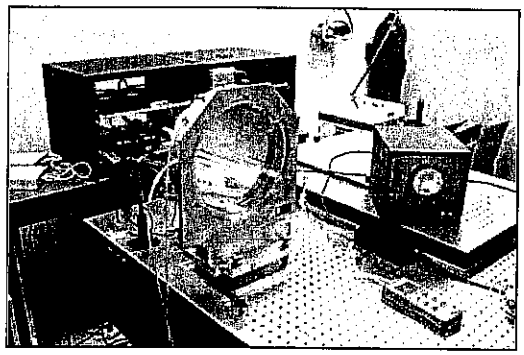

Figure 11. 0.25-meter Membrane Mirror Integrated with Electrostatic Control.

After the electrodes were cut, they were adhesively attached to a plexi-glass support disk. Slots were fabricated on the plexi-glass sheet for the electrode tabs to pass through them. High-voltage leads from the power supply were attached to these tabs using conductive copper tape on the disk side facing away from the membrane. The plexi-glass was supported by a ceramic rod, one end of which was glued to the center of the disk side facing away from the membrane. The other end of the ceramic rod was clamped into a fixture. Because the amount of electrostatic pressure that could be created was dependent on the distance between the membrane and electrode surface, the fixture was designed such that the distance could be adjusted, thus allowing us to vary the distance between the membrane and the electrode surface.

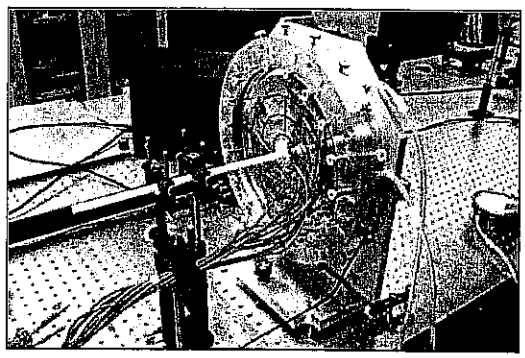

Figure 12. 14-Channel Electrode System and Support Setup.

C. Electrostatic Controller Hardware Development

A fourteen channel electrostatic control system was designed to test the electrostatic control on the small-scale mount. This system is based around a LabView control panel/ data acquisition card controlling a bank of 12 kV high voltage power supplies. Figure 13 shows the high voltage power supplies mounted in a desktop rack system. Power supplies, components and rack setup used for this test were selected based on previous studies. The same setup was used for the 0.70m mount control system as well (additional channels were added).

A LabView control panel, similar to that shown in Fig. 4 was built to control the output voltage for each electrode on the 0.25-meter electrostatic backplane. The panel also provides a proportional master slider to control voltages on all electrodes and also for each ring. To improve control of the high voltage power supplies, the wiring

connectors for the power supplies incorporated the feedback channels and on/off control support. An analog input card added to the computer controller monitors the output voltage from the high voltage power supplies.

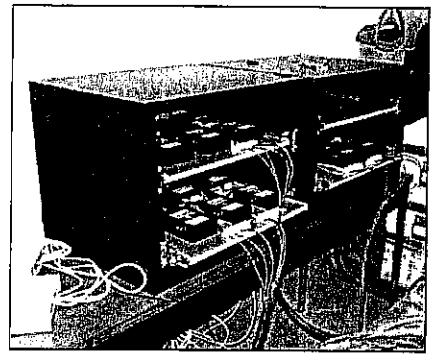

Figure 13 Desktop Racks for High Voltage Power Supplies.

D. Testing

Initial testing of the full aperture control initially focused on adjusting the distance from the mirror vertex and assuring that the backplane was parallel to the membrane. The membrane was then pressurized to obtain the design 1.63m radius of curvature for this small-scale membrane and setup to obtain data using a Ronchi test setup. Figure 14 shows the Ronchigrams and resulting optical path difference (OPD) plot for the membrane with no electrostatic pressure. With the focus term removed this plot shows the characteristic spherical error for an inflated membrane. The electrostatic system was then powered on and adjusted to try and achieve the best shape initially by noting the changes in the Ronchigram. Figure 15 shows the results. The lines in the Ronchigrams are notably straighter out to the edge, a result of reduced spherical aberration. There is some distortion though near the center of the Ronchigram that is due to some irregular peaks in the electrode film. These are located on the tabs that run through the acrylic to make the electrical connection. This can be corrected simply by creasing the electrode tab to make a clean contact between it and the acrylic surface. Nevertheless the resulting OPD shows the improvement in the membrane shape. The spherical aberration has been reduced from 5.9 to -0.6 microns. In this case some spherical error is required for a parabolic surface. Due to some of the electrode plane irregularities there was a slight increase in the astigmatism and some higher order terms. Some of this can be corrected by continuing to adjust the

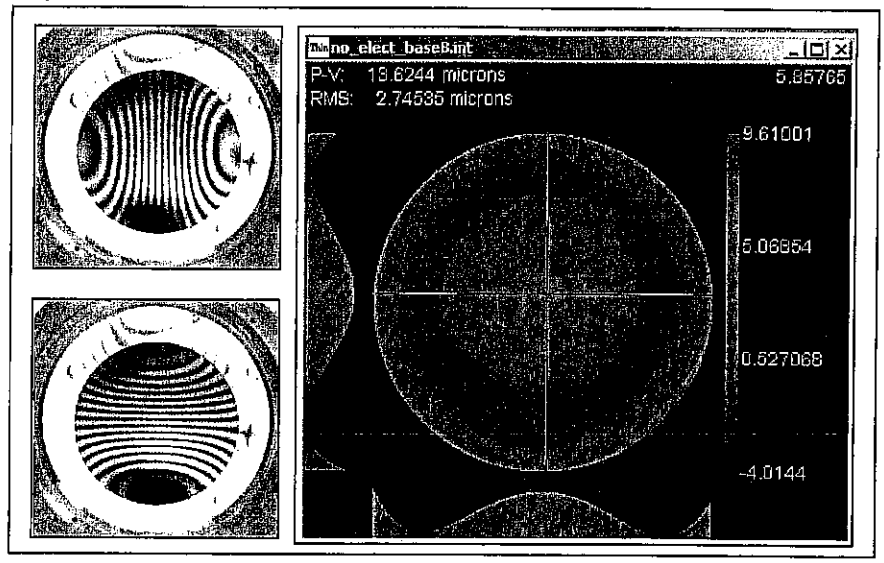

Figure 14. Membrane shape data with no electrostatic pressure.

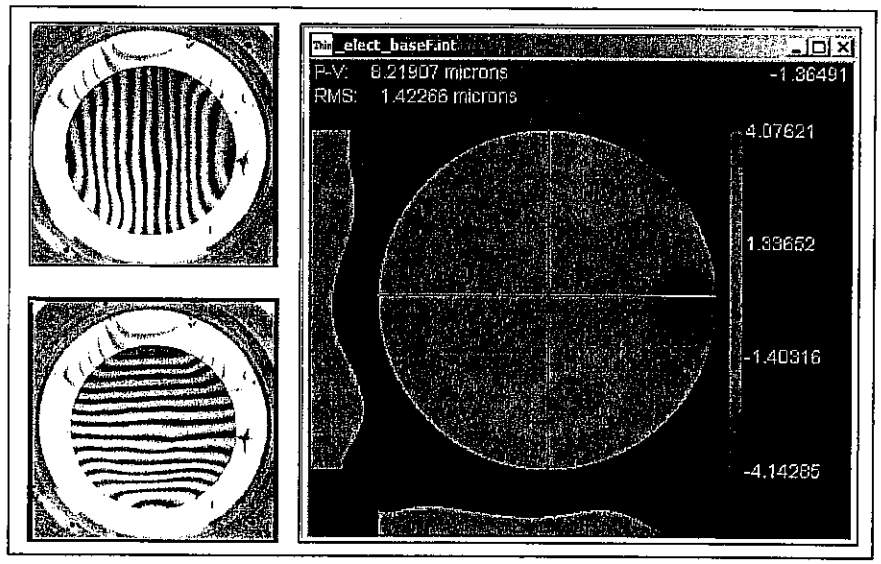

Figure 15. Membrane shape data with electrostatic pressure.

electrodes. This test demonstrated the functionality of the electrostatic control system that was then applied to the 0.70m mirror system only along the boundary.

IV. 0.70m System Testing

A. Uniformly Coated Membrane

Figure 16 shows an inflated membrane system setup at SRS, since the canopy, as well as the mirror, are clear in this case so the surfaces are difficult to see. Figure 17 shows some initial Ronchi test data from the mirror. Some of the errors from the edge limit the useable aperture, however no tuning has been conducted yet to improve this. This testing is currently ongoing, as well as preparations for integration with the electrostatic system.

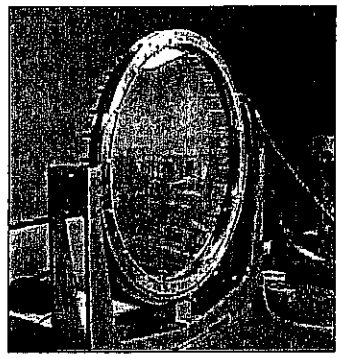

Figure 16. Inflated Lenticular with clear membranes.

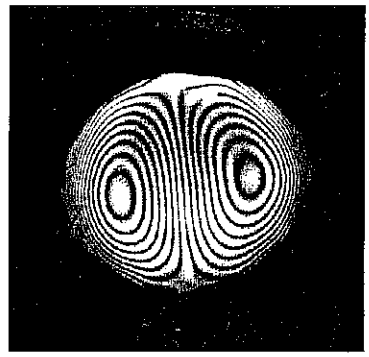

Figure 17. Unadjusted, initial Ronchi data taken from membrane.

A uniformly coated mirror was tested first to provide baseline test data to compare to the varied stress coated mirrors to determine the control over spherical aberration. Figure 18 shows a front and back image of the mount with the uniformly coated membrane in place. Figure 19 shows the initial uncorrected figure error OPD plot for the uniformly coated membrane. As expected spherical aberration is the dominant error. Astigmatism and coma contribute mainly as well. The model predicted pressure to achieve the 62" focal length was 0.037psi with actual coming in very close at 0.035psi.

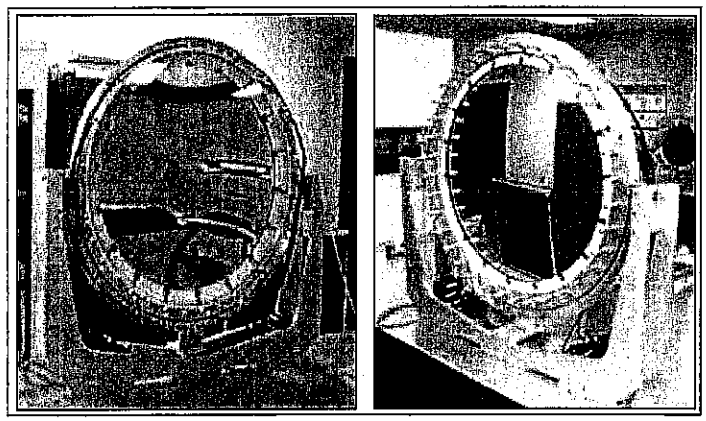

Figure 18. Front and back of assembled membrane mirror mount with uniformly coated membrane.

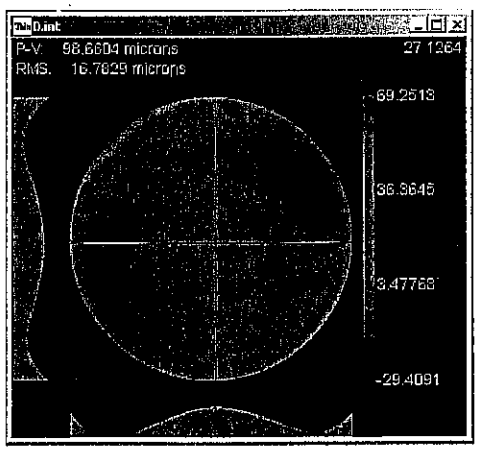

Figure 19. OPD plot of uncorrected uniformly coated membrane mirror shape (focus term removed).

As described earlier two types of control authority over the membrane are available on this mount. They are mechanical micrometer actuators placed normal and in contact to the membrane boundary ring and electrostatic control around the outer perimeter of the membrane (further details are available in previous reports). Testing began by placing the membrane under the Ronchi test and manually tuning the normal actuators until the most symmetric and largest Ronchigram is obtained. Ideally this would reduce some of the initial astigmatism in the mirror. Figure 20 shows the initial Ronchigram and corresponding data for the manually tuned uniformly coated membrane. The analysis area of the membrane had to be apertured down due to the high amount of spherical aberration present (as expected) to be able to obtain meaningful data. This resulted in measuring a 50.8cm diameter area out of the full 70cm usable diameter. As the data shows, spherical aberration is the highest contributor, however, this term cannot be adjusted using

boundary control and therefore will be not be addressed at this point. The varied stress coated membrane should alleviate some of the spherical aberration and will again be discussed when summarizing testing of the varied membrane. The other main contributors are astigmatism and coma. After manually tuning the normal actuators as best as possible, data was handed off to the finite element model and SRS' Integrated Optical Design Analyzer (IODA) which was modified during this effort to include a nonlinear analysis option for better influence function development for the actuators. The data flow for this analysis has been discussed at length previously[4]. The summarized version of this is that shape data is taken from the membrane using the Ronchi test and transferred through IODA, which provides the necessary actuator movements to improve the membrane shape. Using modeled normal actuator influence functions the process was conducted over numerous iterations for only the normal actuators. Figure 21 summarizes this data. The RMS values given in the table do not include the focus Zernike term since it is meaningless in the Ronchi test data. The error is compared to a flat, therefore if the focus term is removed and the shape is a parabola then the error should be much lower. The astigmatism terms and overall RMS decrease with each iteration. The main remaining contributor to this RMS error is the high spherical aberration as well as some first order coma. Figure 22 shows all the Ronchigrams taken of the uniform membrane illustrating the progression of improvement as the normal actuators were tuned. From the data shown in Fig. 21 it is clear that it took several iterations to decrease the error and the astigmatism still was not completely tuned out. The main reason for this is the fact that the full membrane aperture could not be measured due to the spherical aberration. This provided for a varied response for each normal actuator on the shape of the membrane as well as slightly confounding the influence function relation between the finite element

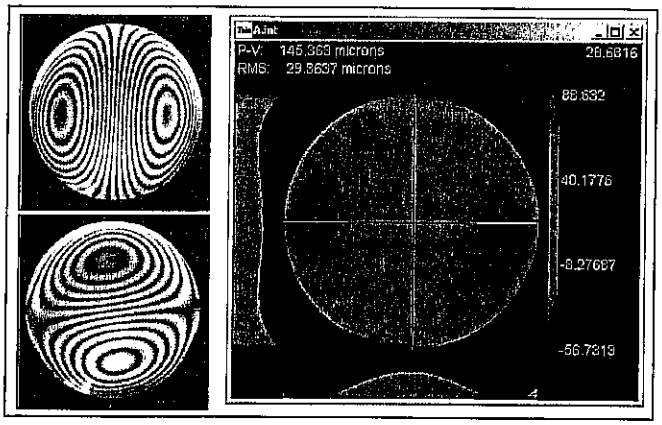

Figure 20. Ronchigrams and data for manually tuned uniformly coated membrane (focus term removed).

Normal Actuator	Iteration (Actuator stoke in microns)						
	1	2	3	4	5	6	7
1	-25.74	49.63	24.85	16.98	-30.31	23.18	16.53
2	-28.58	51.17	26.61	19.84	-16.38	13.48	15.30
3	-29.03	50.04	27.24	21.62	8.35	2.12	9.91
4	-26.68	45.65	26.29	21.78	29.28	-4.65	3.75
5	-21.16	36.39	22.68	19.50	35.13	-4.34	-0.14
6	-12.47	21.05	15.49	14.18	24.57	0.54	-0.98
7	-1.25	0.07	4.69	5.85	5.86	4.52	-0.36
8	11.16	-23.82	-8.39	-4.47	-9.58	3.17	-0.73
9	22.97	-46.34	-21.48	-15.01	-15.05	-3.89	-3.44
10	32.33	-62.98	-32.02	-23.70	-12.17	-12.80	-7.61
11	37.69	-70.42	-37.95	-28.83	-8.18	-18.22	-10.78
12	38.00	-67.33	-38.29	-29.48	-9.45	-17.02	-10.78
13	32.97	-54.39	-33.07	-25.69	-16.09	-10.19	-7.31
14	23.13	-33.87	-23.24	-18.32	-21.93	-1.92	-2.25
15	9.86	-9.00	-10.30	-8.74	-19.54	3.48	1.62
16	-4.75	16.49	3.86	1.51	-6.55	4.52	2.62
17	-18.23	38.82	17.15	10.97	11.79	3.13	1.27
18	-28.35	54.71	27.55	18.42	25.75	2.83	-0.17
19	-33.68	62.11	33.55	23.02	27.89	5.68	0.51
20	-33.90	60.67	34.49	24.38	18.31	10.61	3.78
21	-29.80	51.83	30.78	22.62	4.69	14.10	7.86
22	-22.75	38.14	23.67	18.26	-3.39	12.93	9.96
23	-14.16	22.16	14.67	12.09	-1.41	6.73	8.29
24	-5.01	5.59	5.01	4.93	6.69	-1.52	3.37
25	4.21	-11.00	-4.63	-2.49	11.49	-7.53	-2.25
26	13.17	-27.41	-13.92	-9.54	5.45	-8.76	-5.70
27	21.29	-42.83	-22.41	-15.62	-10.84	-6.27	-5.83
28	27.57	-55.18	-29.12	-20.06	-28.04	-3.85	-3.89
29	30.77	-61.41	-32.62	-22.18	-34.12	-5.08	-2.57
30	29.93	-58.85	-31.62	-21.50	-22.85	-10.31	-3.87
31	24.88	-46.74	-25.71	-17.99	1.00	-15.99	-7.46
32	16.42	-27.05	-15.85	-12.21	23.97	-16.90	-10.72
33	6.11	-4.00	-4.13	-5.19	32.25	-9.87	-10.44
34	-4.32	17.58	7.01	1.89	20.71	3.53	-5.16
35	-13.50	34.15	15.77	8.13	-3.36	17.46	3.62
36	-20.70	44.53	21.54	13.14	-24.85	25.16	12.12
	Initial						
X-Astigmatism (microns)	-61.63	-79.84	-42.39	-30.24	-15.91	-15.68	-10.34	-4.81
Y-Astigmatism (microns)	-15.14	-13.27	-11.6	-11.04	-5.59	-1.76	-3.82	-0.52
RMS (microns)	29.31	35.3	21.69	18.09	16.72	14.41	13.48	13.19

Figure 21. Data summary for normal actuator stroke iterations as provided by modeling data (focus term removed from RMS).

model and the actual test article. It was deemed sufficient at this point to use the modeled normal actuator influence functions over measuring each individual actuator influence. The only difference is it would take more iterations to reduce the overall error to a lesser degree.

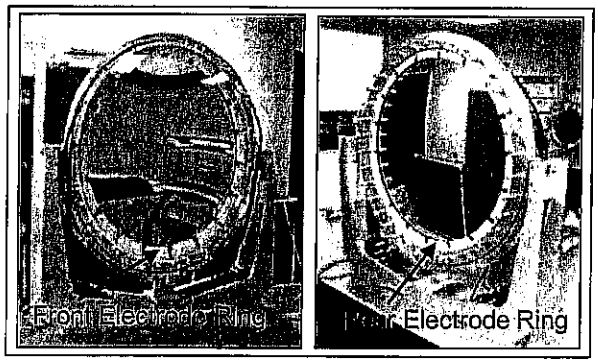

Figure 23. Electrode rings on large membrane mirror mount.

The next step was to test out the electrostatic boundary control system on the large-scale membrane mirror. Figure 23 shows images of the membrane mount with the electrostatic control rings noted. The intent of this system was to mainly take care of any coma error in the membrane. One note to reiterate is that a full aperture electrostatic control system would allow greater control over the membrane shape, but again the point of this program was to attempt to correct the shape as best as possible using only boundary control to help maintain a lower overall areal density potential. From the step 7 tuning result from Fig. 21 the Zernike terms for the x and y coma were 9.48 and -3.48 respectively. Testing of the electrostatic control system began with conducting operations to ensure that there was no arcing within electrode ring and that the assumed voltages from the computer control were being achieved. This went over with no notable errors. The next step proceeded the same as the normal actuators. Data of the shape was taken and input into the finite element model and IODA for adjusted actuator voltage settings. As noted with the normal actuators the fact that the spherical aberration forced a smaller aperture measurement this limited the effectiveness of the actuator/model data exchange. Since the electrostatic response is much more complicated and more confined to the outer edge than the normal actuators this problem was magnified for the electrostatic control. It is more critical to obtain a real measured actuator influence function for the electrostatic response since it can vary more than the ideal modeled response. However, since the measured membrane area had to be apertured down severely due to the spherical aberration this provided a much less effective electrostatic response, due to the fact that the area most effected by it was not measured. This resulted in essentially no model correlation and therefore no reduction in the coma aberration. It should be noted again, however, that the main point of the uniformly coated membrane was to provide the baseline data for comparison to the varied stress coated membrane in terms of spherical aberration. It has been anticipated that the uniformly coated membrane would be limited in correctability due to the spherical term and this is what has been observed.

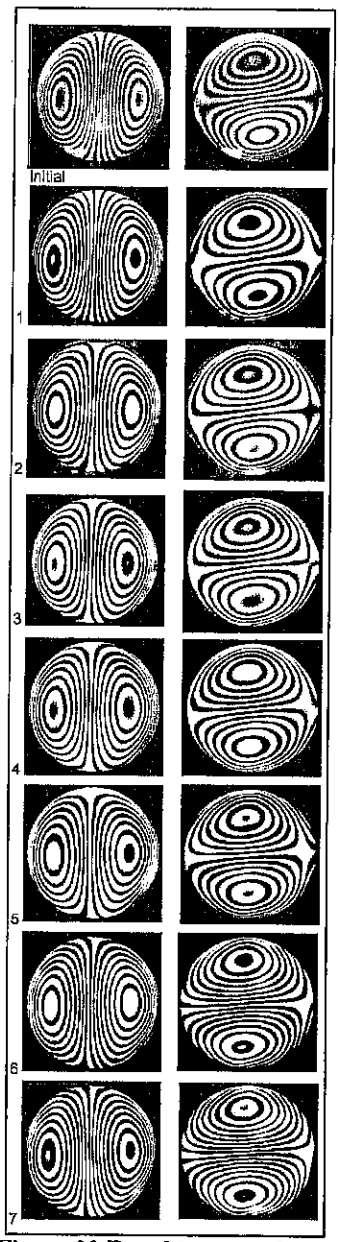

Figure 22 Ronchigrams of uniform membrane with model guided normal actuator tuning.

B. Varied Stress Coated Membrane

Testing of the membranes with a varied stress coating was the next step. Figure 24 shows the mounted membrane revealing the varied stress coating on the back side of the film. To reiterate the point of this coating was to vary the mechanical properties of the membrane so that when inflated it would force the membrane into more of a parabolic shape then a severely spherically aberrated one. Only initial manual tuning was initially conducted, however excellent results were immediately observed. Figure 25 shows a Ronchigram of the membrane after rough

manual tuning of the normal actuators. Comparing this to any of the Ronchigrams shown in Fig. 22 it is clear that there is a dramatic difference in overall shape. One very important note is that the spherical aberration has been reduced to such a degree that the Ronchigram shown is the full usable aperture of the membrane. This is a critical achievement, demonstrating the feasibility of modifying the mechanical properties of the membrane through varied stress coating application. The next step was to use model directed actuator modifications for both normal and electrostatic actuators to reduce the overall shape as much as possible.

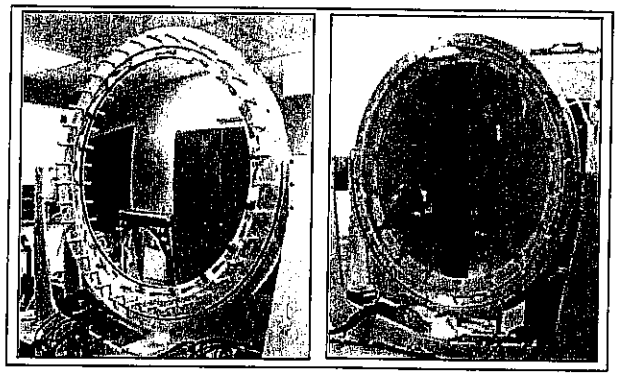

Figure 24 Front and back of assembled membrane mirror mount with varied stress coated membrane.

There were two varied stress-coated membranes that were produced during this effort and were tested, films A and B. Each was coated with the same varied-stress coating distribution. However, the prescriptions between each film were thought to be approximations and would not match exactly due to cost of having a extremely accurate mask fabricated for this process since the coating prescription would most likely not be completely accurate due to some assumptions made of the polymer and coated material properties[4]. Figure 26 summarizes the Ronchigram and corresponding OPD plot (focus term removed, compared to flat) showing the progression of the membrane shape for film A from initial tuning through model directed tuning of the normal actuators. From the data shown the initial PV was 202.61 microns and the RMS was 32.36 microns. After all the normal data actuation was implemented the final PV and RMS was 87.29 microns and 11.44 microns respectively. No improvement using the electrostatic system was achieved on this film, and therefore none is discussed here. The same type of data summary for film B is shown in Fig. 27. While normal actuator tuning provided the majority of the corrections shown the last modification also included electrostatic actuator contributions as well. From the data shown the initial PV was 113.79 microns and the RMS was 17.18 microns. After all the normal data actuation was implemented the final PV and RMS were 60.77 microns and 7.48 microns respectively, both a significant improvement over membrane A. Some of this improvement between films is simply due to better overall tuning with the electrostatic system, but some is inevitably from slight variances between the deposition runs for the varied stress coatings. The data shown for both films is for the entire visible aperture 0.70m in diameter. Since there are some significant edge effects contributing to the calculated error each film was reanalyzed from the best case error reduction using a smaller aperture (0.58m). Figure 28 shows the data for each film using this smaller aperture. While film A winds up providing a slightly better RMS, film B still has a better PV. Both films apertured down, though, had PV and RMS values lowered by approximately one-half over the full aperture.

Figure 25. Ronchigram of varied stress membrane after initial rough normal actuator tuning.

It should be noted that there was some added mirco roughness on some areas of each coated membrane. Some of this is visible in the Ronchigrams as a slightly blurred area, however the Ronchitest can still be administered with no significant shape degradation. It is anticipated that some of this will be picked up during interferometric testing planned at AFRL. The cause of this is can most likely be attributed to several factors. One is dwell time of the evaporative coating source on the film. This film has a much thicker coating than typical for reflective purposes since a different objective was desired (mechanical property adjustment). If the membrane is allowed to get too hot during deposition this can lead to the effect described. Another possibility is the tool-side coating of this material. Typical SRS polymers are coated on the air side for optimum performance. Several areas on the tool side of the membrane that resemble water marks are visible and could be due to coating interaction with the release interface used during polymer production. Regardless, it is not anticipated that this noted issue has severely affected the global shape of the membrane and in achieving the desired effect of mechanical property manipulation of the membrane/coating composite. Additional adjustments to the coating deposition mask and run times, as well as using modifications to the polymer membrane casting substrate surface preparation should help alleviate this issue. The central 15inches of the membranes do not show this effect. It is only noted as you move towards the edge of the film.

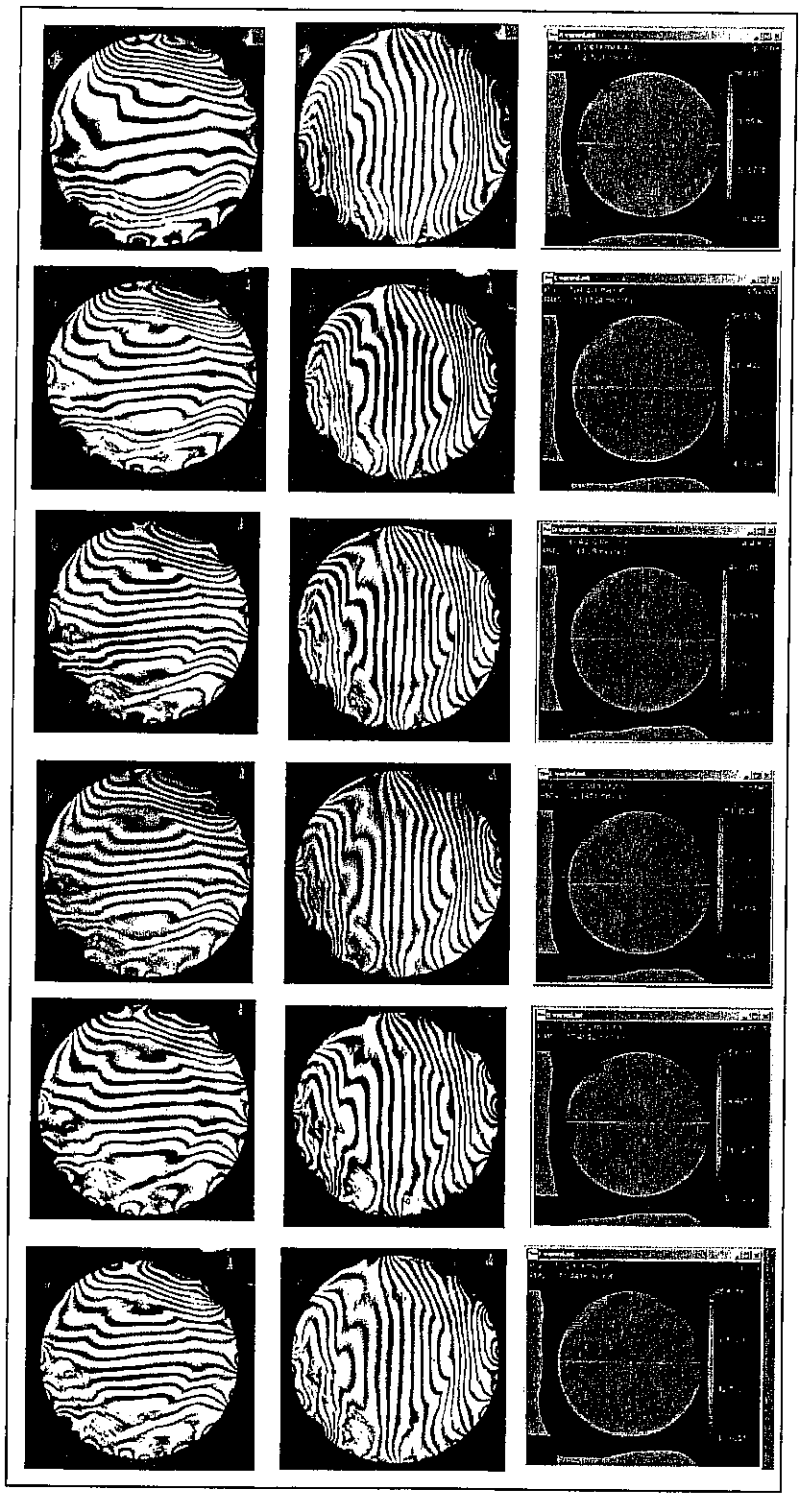

Figure 26. Summary of Ronchigrams and OPD plots for film A (focus term removed from RMS).

V. Conclusions

This study shows that active boundary control can be very effective for correcting certain types of figure errors typically seen in membrane mirrors. Compared to full aperture control, edge control is relatively simple to implement, results in a lower aerial density, and presents no need for a

complex backing structure behind the full aperture. The scaling relationships are also more favorable for boundary control.

Of the configurations evaluated in this study, we found that the best performance was achieved by a design that used a combination of linear displacement actuators, for out-of-plane boundary warping of the membrane support ring, and electrostatic pressure actuators located circumferentially around the outer diameter of the membrane just inside of the boundary support ring. It was obvious that significantly better results could be achieved by controlling two degrees of freedom around the boundary, rather than only one degree of freedom being controlled by either of the types of actuators independently.

While it was shown that boundary control could nearly completely correct astigmatism and coma errors, it was found to be ineffective in correcting the spherical error characteristic of a pressure augmented membrane mirror. In a perfectly static world this would not be a major problem because secondary optics could be used to correct the spherical aberration. However, some degree of correction for spherical error is desirable to correct for off design or incident wavefront errors containing spherical aberrations. The feasibility of varied stress coatings on the membrane has demonstrated that it can reduce the amount of spherical aberration present in the film when pressurized. Additional research and testing can further fine tune this system in order to achieve viable light weight large aperture primary mirrors for imaging applications.

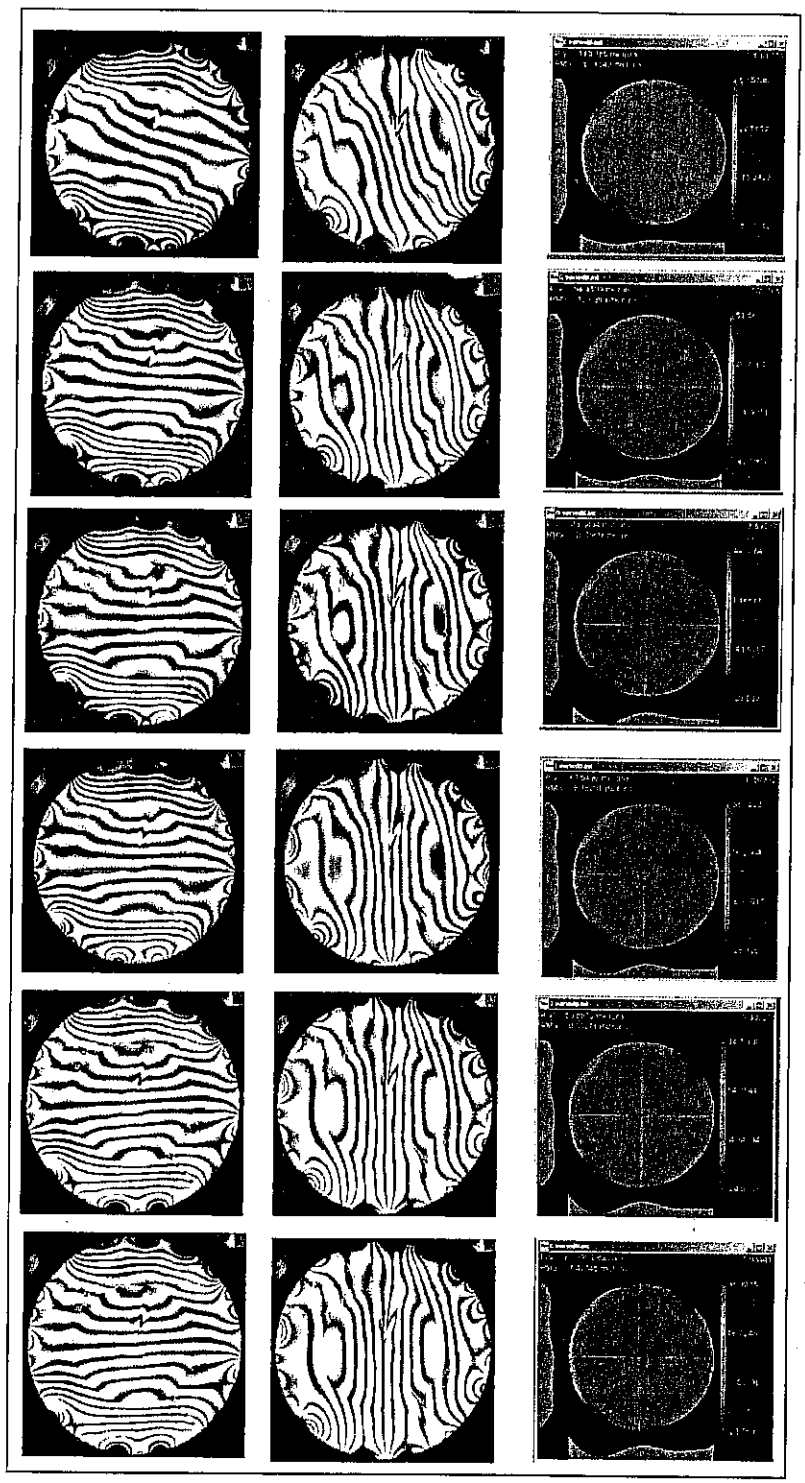

Figure 27. Summary of Ronchigrams and OPD plots for film B (focus term removed from RMS).

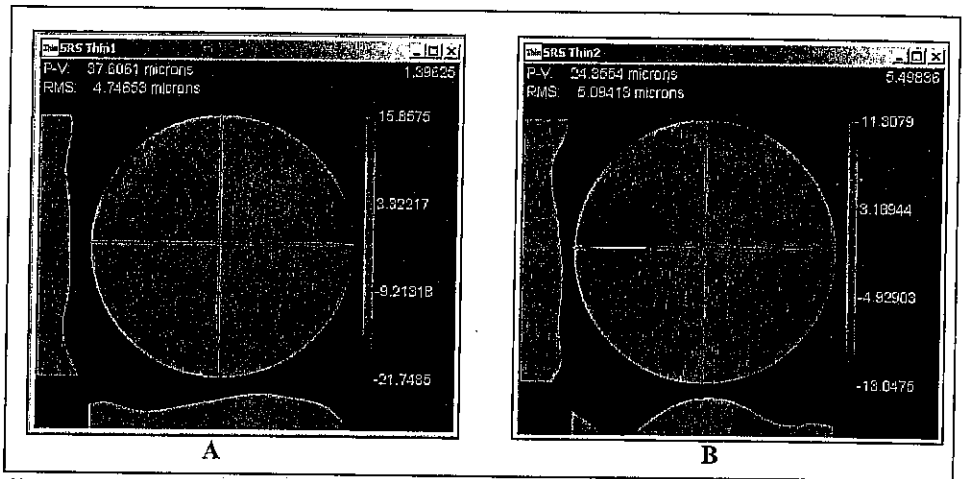

Figure 28. OPD plots for best case data from varied stress-coated films A and B reanalyzed with the aperture reduced from a 0.70m to a 0.58m diameter.

Acknowledgements

This work is supported by the Directed Energy Directorate of the Air Force Research Laboratory, under contract F29601-03-C-0040.

References

[1]Murphy, L.M., Tuan, C. "The Formulation of Optical Membrane Reflector Surfaces Using Uniform Pressure Loading", Contract Report, SERI/TR-253-3025, 1987.

[2]Clayton, W.R., Gierow, P.A., "Inflatable Concentrators for Solar Thermal Propulsion", ASME Solar Engineering, 2, , 1992, pp. 795-800.

[3]Patrick, B.G., Moore, J.D., Marker, D., Rotge, J., "Polymer Material and Casting Process Development for Reduced Manufacturing Cost of Spaceborne Optics", Proceedings of SPIE, Vol 5179, Optical Materials and Structures Technologies, 2003.

[4]Patrick, B, Moore, J., Maji, A., Marker, D., Wilkes, M., "Meter-Class Membrane Mirror with Active Boundary Control", Proceedings of AIAA-2005-2193, 2005.

[5]Moore, J., Troy, E., Patrick B., Stallcup M., "Software for Integrated Optical Design Analysis", Proceedings of SPIE, Vol 4444, 2001.